VERSITA

OPTO-ELECTRONICS REVIEW **15**(2), 102–109

DOI: 10.2478/s11772-007-0006-8

Investigation of limitations of optical diffraction tomography

T. KOZACKI*, M. KUJAWIŃSKA, and P. KNIAŻEWSKI

Institute of Micromechanics and Photonics, Warsaw University of Technology, 8 Św. A. Boboli Str., 02-525 Warsaw, Poland

Optical diffraction tomography (ODT) applied to measurement of optical microelements is limited by low dynamic range, i.e., only objects with small deviations of refractive-index distribution can be measured. Therefore in this paper the limitations and errors of ODT are investigated throughout extensive numerical experiments. It is shown that these errors can be reduced by introduction of additional numerical focusing in the tomographic reconstruction algorithm. Additionally, new tomographic reconstruction algorithm using back propagation in reference medium for optical microelements measurement with known design is proposed. This hybrid reconstruction algorithm allows significant extension of ODT applicability in measurement of elements having large deviations of refractive-index distribution.

Keywords: optical diffraction tomography (ODT), propagation in inhomogeneous media, fiber optics characterization.

1. Introduction

Optical diffraction tomography (ODT) [1] is the method for characterization of 3D distribution of material parameters in an optical element. This includes refractive-index and absorption or birefringence. However, there are limitations of ODT applicability, only the elements having homogenous structures can be accurately characterized. Therefore in the paper we study the errors of reconstruction limiting the application of ODT to nonhomogeneous structures. We also show that using a priori knowledge about an object structure, these errors can be reduced.

In the presented study we employ the standard ODT experimental configuration [2–4] shown in Fig. 1(b) where the object angular orientation relative to the incident plane wave is changed sequentially in the range from 0° to 360°. For every rotation angle φ, the object projection images P_φ (integrated phase and integrated amplitude) [Fig. 1(a)] are captured by means of interferometry [5] (including holography [6]). In order to properly reconstruct an object internal structure, the captured projection images must well approximate object integrated phase and amplitude distributions. This condition is met if the object structure variations are small comparing to the wavelength and light propagates nearly along straight lines. It is much easier to fulfil the above condition if the projection images are captured in the system shown in Fig. 1(b). Here, the optical system images the centre of an object in the detection plane. In such a case, the captured projected image data are distorted by the object internal refraction or diffraction only. Nevertheless, the strong object internal refraction or diffraction meaningfully distorts the projected images giving incorrect reconstruction.

Using a procedure described above, several experiments for variable angular orientation of object are performed producing a set of integrated amplitude and phase

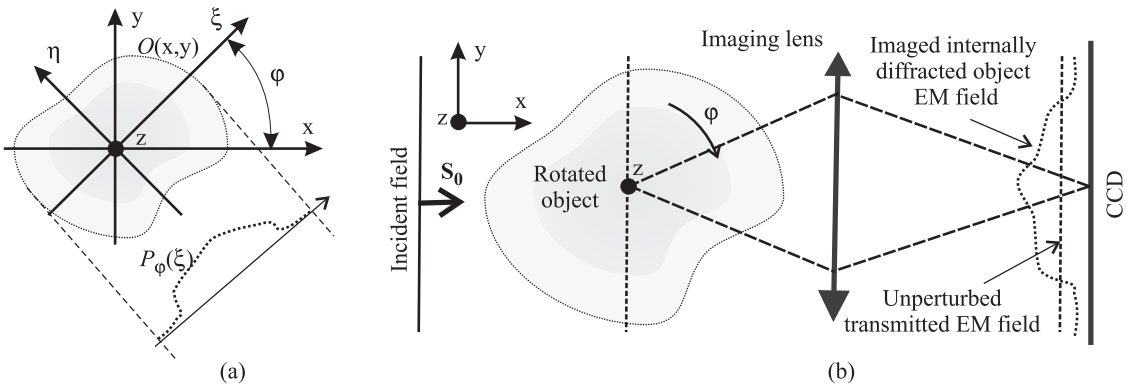

Fig. 1. Coordinate system with geometry defining object projection (a) and the scheme of a standard data acquisition system of ODT (b).

*e-mail: t.kozacki@mchtr.pw.edu.pl

maps. Below, we will consider ODT in the application of refractive-index distribution studies only. In such a case, the measurements of integrated phase by means of interferometry are performed. To reconstruct the object internal structure of refractive-index $O(x,y)$, one of tomographic reconstruction algorithms such as filtered back projection algorithm (FBP) [7] can be used

$$O(x,y) = \frac{1}{(2\pi)^2}\int_0^{\pi} d\varphi \int_{-\infty}^{\infty} |\mathbf{k}|\widetilde{P}_{\varphi}(\mathbf{k})\exp\{i\mathbf{k}(x\cos\varphi + y\sin\varphi)\}d\mathbf{k}, \quad (1)$$

where

$$\widetilde{P}_{\varphi}(\mathbf{k}) = \int_{-\infty}^{\infty} P_{\varphi}(\xi)\exp\{-i\mathbf{k}\xi\}d\xi, \quad (2)$$

is the Fourier transform of the projection P_{φ}.

Using FBP algorithm, the two dimensional (2D) cross sections (for one z value) of internal object structure are reconstructed. By successive stacking of the reconstructed 2D distributions, a full three-dimensional structure of an object is recovered.

Similar measurement scheme is applied in the technique known as photoelastic tomography for determination of an object internal distribution of the birefringence [4,8]. The only difference is that the integrated projection images of birefringence are measured using integrated photoelasticity [4,7]. In this case, the same errors appear due to object internal refraction and diffraction. Therefore the paper analysis is equivalently valid for both diffraction and photoelastic tomography.

There are many tomographic reconstruction algorithms and all of them require linearization of the light interaction with an object neglecting significant internal diffraction or refraction. Several techniques are known for linearization of this process including assumptions that optical radiation propagates along straight lines, the inverse scattering approximations or Bouguer's formula [1]. The algorithms of computerized tomography [8] used in the case of the first technique are, the mentioned above FBP algorithm or Abel transform for axisymmetric objects [9]. The reconstruction algorithms, that accounts for diffraction using the Born or the Rytov weak-scattering approximations, are the filtered back propagation algorithm [10] and recently developed the distorted wave Born approximation algorithm (for axisymmetric objects) [11]. Algorithms using third linearization technique are developed for axisymmetric objects, however, extensions of the technique for arbitrary objects are available using iterative techniques [12]. Nevertheless these algorithms can be used if an object is characterized by monotonic distribution of refractive-index only.

Major drawback of ODT applicability in measurement of micro optical elements refractive-index structure is low dynamic range, refractive-index structures with small variations can be measured only. This is due to the significant errors produced by using the mentioned above simplification in the reconstruction algorithms. The paper is devoted to study such errors.

Section 2 of the paper is devoted to numerical analysis of reconstruction errors received due to application of tomographic reconstruction algorithm. In sec. 3, we show that for the object having weak diverging or converging properties the reconstruction error can be reduced by modification of the position of imaging plane. The hybrid reconstruction algorithm allowing significant extension of ODT applicability for the measurement of elements having high variations of refractive-index is presented in sec. 4.

For presentation simplicity in the paper, the numerical analyses are performed for axisymmetric structures. However, all presented methods can be applied for arbitrary objects. In the paper, two types of objects representing most common micro-optical structures in fibers are considered:

- single phase variation structures, e.g., fibers with gradient and step-index core,
- periodic phase variation objects, e.g., photonic fibers with the channels filled with gradient or step index media.

Often the term 'reconstruction' is used alone and refers to 'reconstruction of refractive-index distribution'.

2. Reconstruction errors in optical diffraction tomography

In the experimental tasks, where 3D transparent or semi-transparent specimen is inspected optical diffraction tomography is widely used. Unfortunately, in ODT of microelements, the features size of refractive-index distribution is often of the order of several wavelengths. This causes strong diffraction effects, and ultimately the objects having small deviation of refractive-index can be measured only. In ODT, two algorithms are the most widely used for reconstruction of arbitrary 3D refractive-index object distributions. First, the algorithm uses assumption that optical radiation propagates nearly along straight rays. Numerically it was shown that in this case the most accurate reconstructions are obtained, if instead of scattered field the projection image of the object centre is measured [3]. The second reconstruction algorithm that accounts for diffraction using either Born or Rytov weak-scattering approximations is the filtered back propagation algorithm [10]. The most accurate reconstruction can be received by hybrid filtered back propagation algorithm, in which prior to application of filtered back propagation algorithm, an optical field scattered at an object is numerically propagated back to the object centre [13]. However, through numerical simulations and experiments it was shown that both above mentioned reconstruction algorithms give the results with comparable accuracy. In Ref. 3, quantitative study of 3D reconstruction precision was presented for step-index optical fiber only. Therefore in this section we present the results of extensive numerical experiments for both, step and gradient-index optical fibers with refractive-index variations Δn and with

two diameters. In these numerical experiments, the efficient wave propagation method [14] is applied. It gives the results with comparable accuracy as for previously used [15] rigorous finite-time domain method [16]. It was shown numerically that reconstruction diffraction errors in both tomography of single component dielectric tensor distribution and refractive-index distribution are the same for relatively large deviations of dielectric tensor components. Therefore our analysis presented here is valid for both applications.

To study the errors of refractive-index reconstruction, the numerical tomographic experiments for axisymmetric objects were performed [Fig. 1(b) and (2)]. In such an experiment, a plane wave is illuminating inspected optical structure and received scattered field imaged to the object centre is used as input data for reconstruction. Both mentioned above reconstruction algorithms give the results of comparable accuracy, therefore numerically more efficient algorithm consisting of numerical refocusing (numerical back propagation) to the object centre and tomographic reconstruction based on Abel transform was used.

2.1. Error analysis for simple phase variation objects

The numerical experiments for both step-index and gradient-index (parabolic distribution) optical fibers with two diameters $2r_0 = 10\lambda$ ($\lambda = 0.6328$ μm) and $2r_0 = 100\lambda$ (Fig. 2) were performed. For gradient-index object, the FWHM (the full width at half maximum) parameter was used as a diameter. In all the numerical analyses, the index of refraction of cladding medium is $n_{surr} = 1.46$. The refractive-index variations Δ_n were taken in the range 0–0.1 with the step 0.001. Reconstructed refractive-index distribution n_{rec} was compared quantitatively with the assumed object n_{ob} via equation

$$\Delta_{nerr} = \frac{1}{N} \sum_{|r|<2r_0} [n_{ob}(r) - n_{rec}(r)]^2, \qquad (3)$$

giving the refractive-index reconstruction error Δ_{nerr}. In Fig. 3, the exemplary reconstructions and the received errors as a function of the refractive-index variation Δ_n are presented.

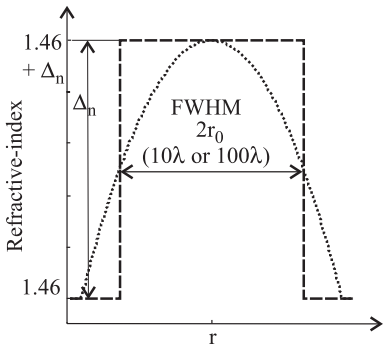

Fig. 2. Exemplary distributions of refractive-index, step and gradient-index.

The errors obtained for step-index object are substantially larger. This effect is related to significant errors at object refractive-index discontinuity, what is especially evident for step-index object of small dimensions (width 10λ). Therefore in this case tomography can be used for $\Delta_n < 0.01$ (approx.), and even then, the received result is an estimate. For larger step-index object (width 100λ), the technique can be used in the wider range, $\Delta_n < 0.03$ (approx.). Moreover, the largest errors are located in the neighbourhood of discontinuity, giving good reconstruction far from it [Fig. 3(a)]. For $\Delta_n > 0.034$, the object discontinuities manifest in errors of phase unwrapping making impossible reconstruction of the refractive-index distribution even at the object central part. This problem refers to low value of intensity at the object discontinuity of imaged projections. Errors received for the gradient index object are substantially smaller. Additionally, in this case there is no error fluctuations, reconstruction errors are distributed more evenly over the object [Fig. 3(b)]. The highest errors are observed in the places where the object refractive-index distribution has the second derivative maximum. Therefore in gradient-index case maximum errors are located at $r = 0$ and $r = r_0$. For example, for $\Delta_n = 0.1$ the error at the centre equals 0.0032 (10λ) and 0.0034 (100λ), while the overall statistical errors are approx. half of that, $\Delta_{nerr} = 0.0021$ (10λ) and $\Delta_{nerr} = 0.0019$ (100λ).

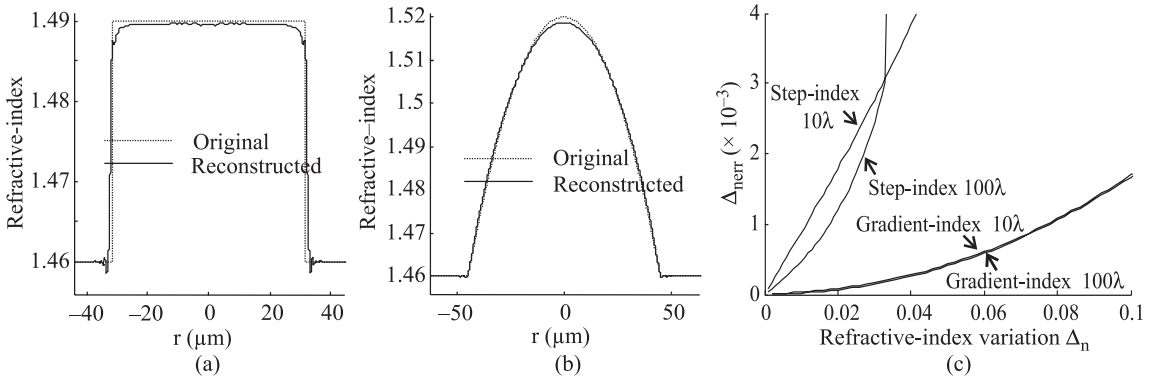

Fig. 3. Exemplary refractive-index reconstruction for the step-index fiber with $\Delta_n = 0.03$ (a), exemplary refractive-index reconstruction for gradient-index fiber with $\Delta_n = 0.06$ (b), and errors of tomographic reconstruction for fiber having step and gradient-index distributions (c).

 © 2007 SEP, Warsaw

2.2. Error analysis for periodic phase objects

Next, the simulations for objects having more complex axisymmetric distributions: cosine and periodical step index with total diameters 100λ were performed. Both distributions have the period $T = 28.57\lambda$. In Figs. 4(a) and 4(b), the object refractive-index distributions and corresponding exemplary reconstructions are shown. The numerical experiments were performed for various values of the parameter Δ_n. The received reconstruction errors were computed (Eq. 3) and plotted in Fig. 4(c). Errors for step-index object are similar to the errors received in the previous analysis. As for the step-index case the method can be applied for the cases $\Delta_n < 0.03$ (approx.). In Fig. 4(b), it is visible that reconstructions for cosine object are characterized by smaller values and slightly distorted period when compared with the original. The allowed refractive-index variations for the gradient case are up to $\Delta_n = 0.1$ (approx.).

3. Improving accuracy by selecting best focus plane

It was proven, that the most accurate results are received if prior to application of tomographic reconstruction the optical field is imaged to an object centre either via imaging system or numerically [2,3]. For such configuration the measured object integrated phase distribution is most similar to the theoretical object projection of a phase. However, for some cases of practical interest, more accurate reconstruction can by received if an optical field is imaged to a plane different than the object centre. Such cases are met if the measured optical structure has weak light converging or diverging properties. To study this feature we have performed tomographic simulation for the objects having composite distributions, step-index with periodic step-index variations (SIP) and gradient-index with periodic step-index variations (GIP). These distributions are composed from light converging refractive-index distributions, step or gradient index and periodic step-index distribution with $\Delta_{np} = 0.005$. Application of such composed distribution allows us to study both reconstruction errors, global and local ones. Global errors can be seen in Fig. 3(a) and 3(b), where it can be observed that the received reconstruction are mainly smaller than theoretical ones. The local errors are shown in sec. 2.2 where the structures with slightly distorted period are reconstructed comparing to the original one. Both distributions SIP and GIP are shown in Figs. 5(a) and 5(b) using a dotted line. In our experimental practice, the best results of reconstruction were received if an optical system is imaging the plane having minimal deviations of intensity, 'best focus' plane [17]. The location of this plane differs from the object centre in the analyzed case of the converging and diverging objects. Therefore we propose below the new reconstruction algorithm with the modified focusing.

In such an algorithm, at first the complex optical field is experimentally established via imaging system in the central plane of a rotated object. Next, using free-space numerical propagation algorithms the optical field is sequentially imaged to the parallel planes inside the object area searching for a plane with minimal deviation of intensity distribution ('best focus' plane). Finally, for this particular plane the integrated phase is computed forming one data set for a given angular object orientation. Repeating this procedure for a number of angular object orientations gives the data set necessary for reconstruction of internal refractive-index structure.

The results of reconstruction using the modified focusing for exemplary SIP and GIP distributions are shown in Figs. 5(a) and 5(b) (solid line). For the step-index case, the focus plane position was modified by defocus (distance from object centre to new focus plane) equal to 3.23 μm ($\sim 0.1 r_0$), while in the case of gradient object by 4.5 μm ($\sim 0.14 r_0$). To visualize the positive effect of focusing modification in Figs. 5(c) and 5(d), the differences between original and reconstructed distributions for both algorithms using standard and modified focusing are plotted. As it is mentioned in sec. 2, the reconstructed distributions of refractive-index are slightly smaller than the original one. Application of the focusing modification in the reconstruc-

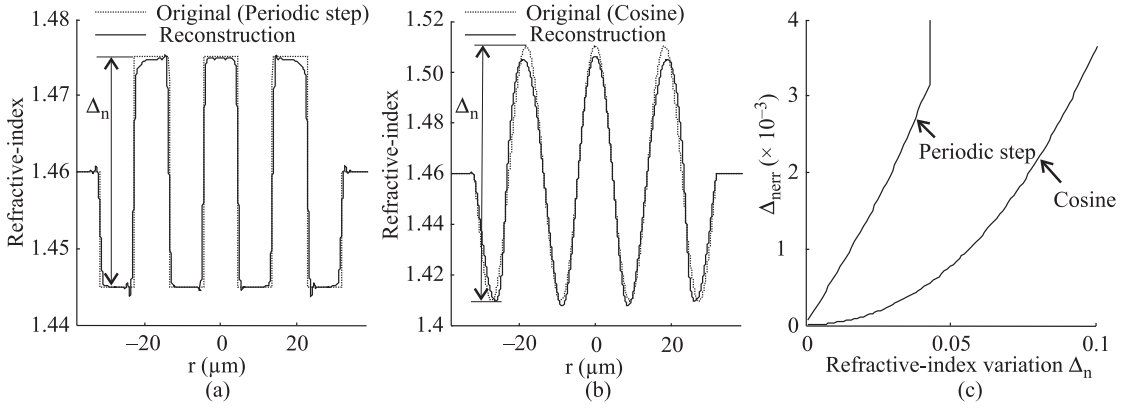

Fig. 4. Exemplary refractive-index reconstruction for periodic step-index object distribution for $\Delta_n = 0.03$ (a), exemplary refractive-index reconstruction for cosine-index object distribution for $\Delta_n = 0.1$ (b), errors of tomographic reconstruction for objects with diameter 100λ having periodic step-index and cosine-index distributions (c).

tion algorithm minimizes that difference (reduction of global reconstruction error) and in addition the period of reconstruction is more close to the original one (reduction of local reconstruction error).

In order to prove more generally, that the focusing modification gives substantial error reduction of object refractive-index reconstruction, the series of simulations for the mentioned above profiles SIP and GIP for variable Δ_n and $\Delta_{np} = 0.005$ were performed. For each object both reconstruction algorithms were applied, the standard algorithm (focusing at the object centre) and the algorithm with proposed focusing modification ('best focus'). In each case, the reconstruction errors were computed using Eq. (3) and they are presented in Fig. 6(a) (SIP) and Fig. 6(b) (GIP). It is evident from both plots that for all simulations the reconstruction errors received using standard focusing method ('dotted line') are substantially larger then those received by the 'best focus' method ('dashed line'). For example, for the object shown in Fig. 5(a), the reconstruction using standard focusing gives the error $\Delta_{nerr} = 0.0019$ while using the modified focus $\Delta_{nerr} = 0.0014$. Similarly, for an exemplary object in Fig. 5(b), the application of modified focus gives 14% reduction of the computed errors $\Delta_{nerr} = 0.00091$ ('centre focus') and $\Delta_{nerr} = 0.00079$ ('best focus'). If the errors would be calculated excluding refractive-index discontinuities or there would be no discontinuities, the error reduction would be even higher. Additionally, for step-index object, the cases for $\Delta_n > 0.034$ can be successfully reconstructed using modified focusing while it is not possible applying standard method. In Figs. 6(a) and 6(b), the values of applied focus modification are plotted using solid line.

4. Algorithm using back propagation in reference medium

Major disadvantage of optical diffraction tomography is low dynamic range, i.e., the objects having small deviation of refractive-index can be measured only. Fortunately, large range of immersion fluids exists and allows us to match the object refractive-index. Nevertheless, there are many micro optical elements having considerable variations of internal refractive-index structure, fiber optics, grin lenses, liquid-crystal devices, etc., that require higher dynamic range. In the recent papers [18], the new method for dealing with these problems was presented, namely distorted wave born approximation (DWBA) method. In these papers, the DWBA algorithm is used to reconstruct elements with axisymmetric refractive-index distribution. In most of the cases we have the knowledge about the expected refractive-index distribution in an optical structure from its design. Due to fabrication errors, real structures are somehow different from their design. Therefore the object in practice is composed of both, overall known struc-

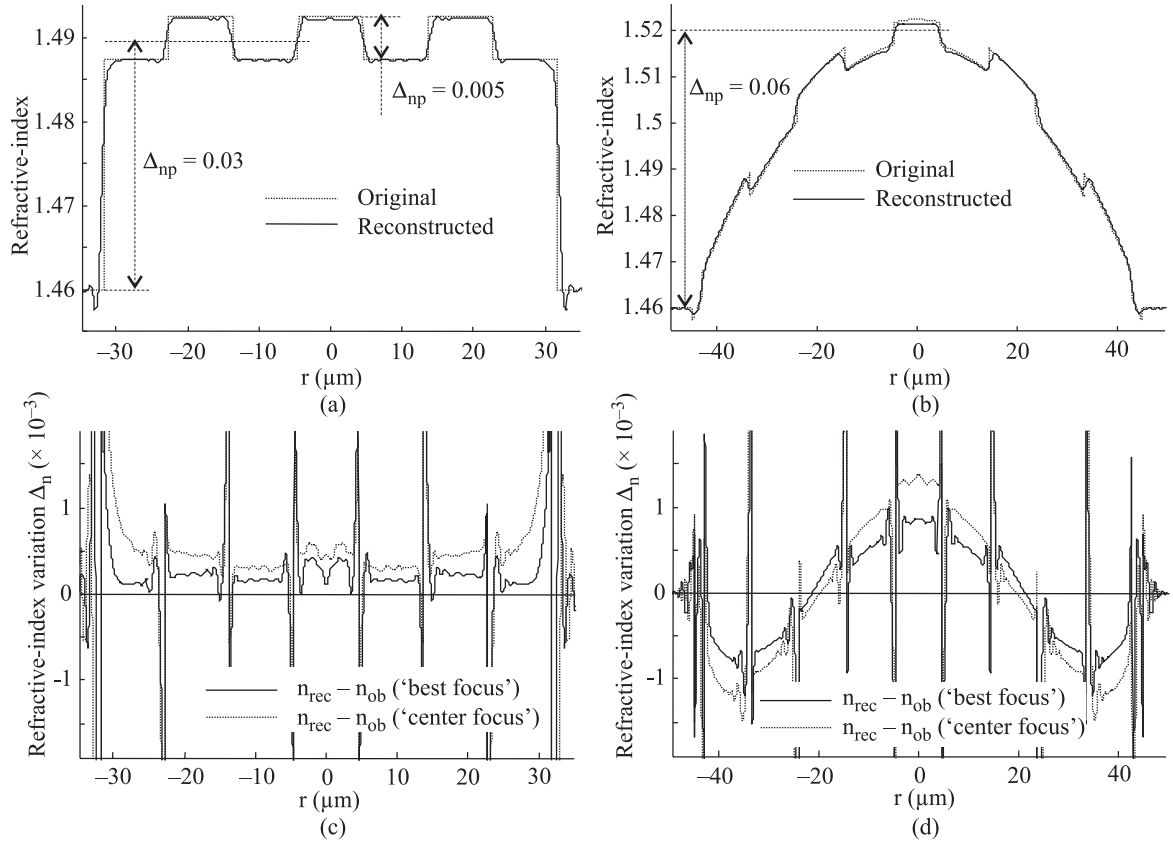

Fig. 5. Reconstruction for SIP profile of refractive-index for $\Delta_n = 0.03$, $\Delta_{np} = 0.005$ ($2r_0 = 100\lambda$) (a), reconstruction for GIP profile for $\Delta_n = 0.06$, $\Delta_{np} = 0.005$ (FWHM = 100λ) (b), error of reconstruction for object in Fig. 4(a) (c), and error of reconstruction for object in Fig. 4(b) (d).

 © 2007 SEP, Warsaw

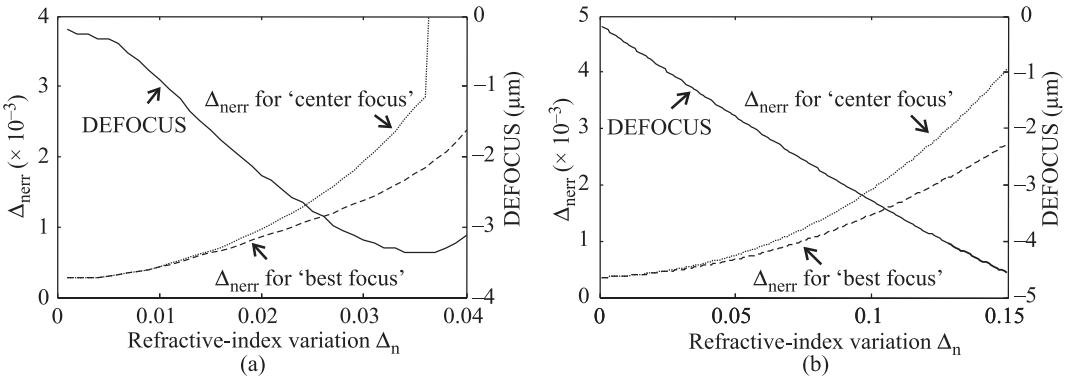

Fig. 6. Reconstruction errors Δ_{nerr} received using standard and modified focusing for SIP objects ($\Delta_{np} = 0.005$) (a) and the reconstruction errors Δ_{nerr} received using standard and modified focusing for GIP objects ($\Delta_{np} = 0.005$) (b).

ture (referred here as 'design') and variation from this known structure (named as 'design deviations'). Implementation of the knowledge about design in ODT can highly extend its dynamic range, because the design deviations are reconstructed only. In Ref. 18, the DWBA method was used to reconstruct optical structure deviations from its design, but the presented method works if both the design and its deviations have axisymmetric distributions.

There are many microobjects which do not fulfil axisymmetric requirement (waveguides, optical structures imperfections). Therefore in this section the modification of the standard reconstruction algorithm is proposed, in which the knowledge about the optical structure design is applied. Thanks to this modification, the design deviations are reconstructed only and structures with high deviation of refractive-index distribution can be measured. The proposed algorithm is relatively fast and simple in implementation. It consists of two major stages, in the stage one, the measured scattered optical field from an object is back propagated through the optical medium of known design, in the stage two, the standard tomographic algorithms are applied [Eqs. (1) and (2)]. The first stage has to deliver accurate projections of the design deviations $P_{\varphi(dev)}$ only.

Since the measured scattered optical field from optical structure contains information about both, structure design and its deviations, the information about design must be removed in the stage one of the algorithm. This is accomplished in a few steps. First, the measured scattered field from an optical structure is back propagated through the structure design medium using the wave propagation method. Next, this optical field is imaged to the object centre, since ODT in the object centre produces most correct projection images (integrated phase distributions). Unfortunately, if the structures have large gradients of refractive index distributions, high nonlinearity occurs in the process and nonlinearly distorted projection images of the design deviations are received. However, we have found, that this nonlinearity causes that the computed projections in the second step is just nonlinearly magnified (magnification is spatially variant) version of the actual projection of the object design deviations $P_{\varphi(dev)}$.

This nonlinear magnification can be found by additional numerical procedure (step three). The procedure consists of a few phases:

- plane wave is propagated in a structure which is a slightly modified version of an object design,
- the obtained optical field is back propagated in object design medium,
- the received optical field is imaged to the object centre giving nonlinearly magnified projection images of introduced deviations,
- by analysis of the theoretical projection and the received magnified one through numerical process the final nonlinear magnification is found through numerical process,
- the determined nonlinear magnification is applied in the stage one of the algorithm and final projection of object design deviation is recovered $P_{\varphi(dev)}$.

Below, some implementation problems and thorough numerical analysis of the errors of this algorithm application are presented. Two composite optical element structures were chosen to study algorithm accuracy:

- step-index design ($\Delta_n = 0.1$) with periodic step-index deviations representing fabrication errors ($\Delta_{np} = 0.01$, $T = 28.57\lambda$), Fig. 7(a) (dotted line),
- gradient-index design ($\Delta_n = 0.2$) with periodic step-index deviations representing fabrication imperfections ($\Delta_{np} = 0.01$, $T = 28.57\lambda$), Fig. 7(b) (dotted line).

The total refractive-index reconstructions are shown in Figs. 7(a) and 7(b) (solid line), while in Figs. 7(c) and 7(d) the reconstructions of periodic structure considered as manufacturing imperfections are presented. In both cases, the reconstructions are very close to the originals. However, an important issue must by pointed out. Close to the structure design discontinuity, the substantial reconstruction error appears. This is evident in both cases in Figs. 7(c) and 7(d). This error comes from the fact that the optical field received from propagation through the design medium is highly distorted by presence of very large refractive-index discontinuity. It is especially visible for the case here examined, where the object has light converging properties. In such cases, the large intensity drop at the refrac-

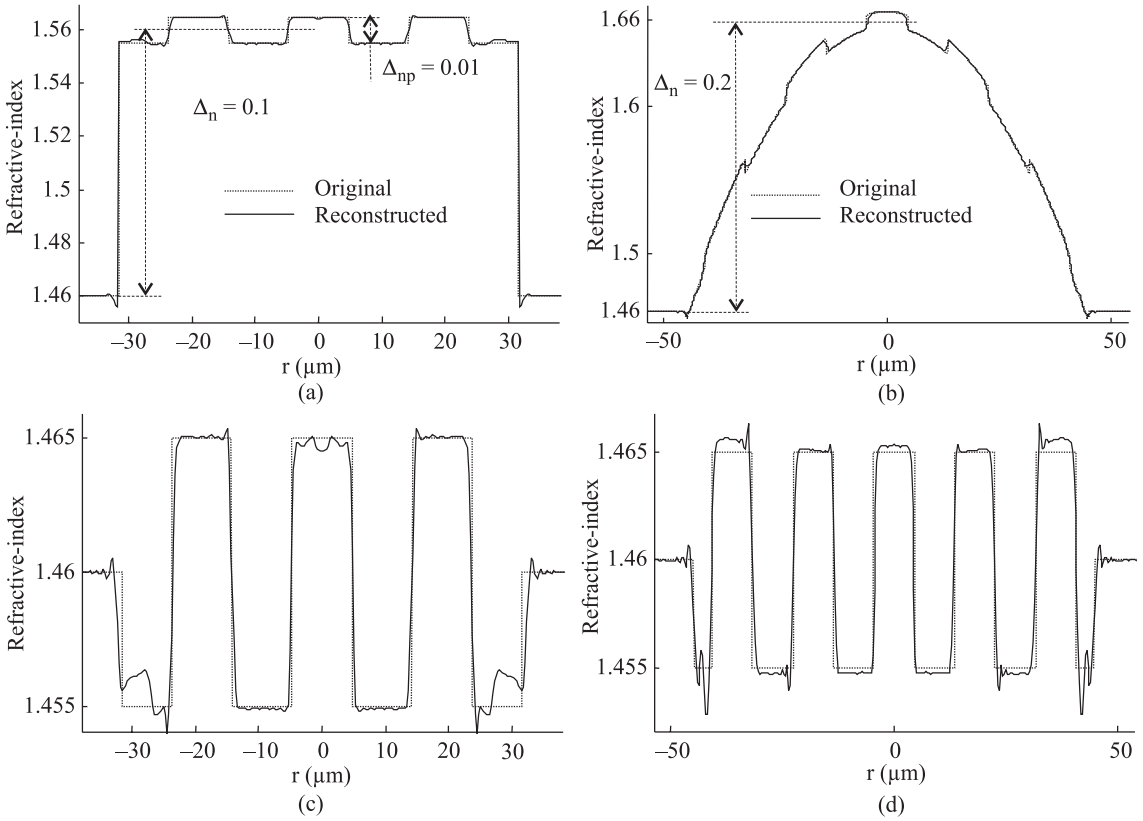

Fig. 7. Exemplary reconstructions received for the algorithm using back propagation in reference medium: reconstruction of the object refractive-index (a), reconstruction of refractive-index deviation from step-index object design (c), reconstruction of the object refractive-index (b), and reconstruction of refractive-index deviation from gradient-index object design (d).

tive-index discontinuity is observed. Therefore the optical structure design modulations at these places cannot be recovered.

As it can be seen in Fig. 7, for both optical structure design cases, the highest errors are located at the area of the structure design discontinuity. Therefore exclusion of this area from the error computations would give meaningful reduction of the computed errors. For example, exclusion of 20% area around design discontinuity for the case presented in Fig. 7, gives following statistical error reduction, 17% reduction for step-index design and 21% for gradient-index design. To get quantitative results of the received errors for the presented reconstruction algorithm, the series of simulations for the above mentioned structure designs (step-index and gradient-index) with the variable Δ_n in the range (–0.21–0.21) and $n_0 = 1.46$ were performed. In these simulations, the analyzed object designs were distorted by periodic step-index and cosine index distributions with $\Delta_{np} = 0.01$ and the period $T = 28.57\lambda$. In all simulations, the statistical errors Δ_{nerr} (Eq. 3) were computed and the received results are plotted in Fig. 8. From both plots it can be clearly seen that the presented method gives accurate reconstructions.

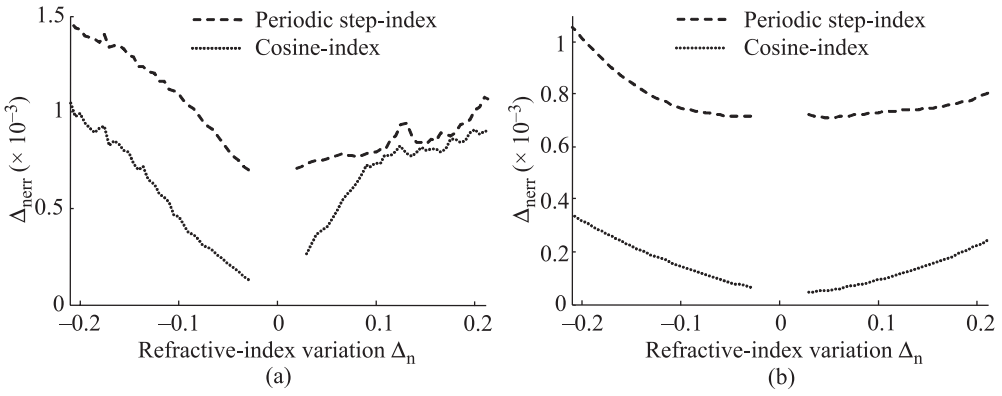

Fig. 8. Errors of tomographic reconstruction using back propagation in known reference medium for: step-index (a) and gradient-index object designs modulated by periodic step-index and cosine-index distributions with $\Delta_{np} = 0.01$ (b).

 © 2007 SEP, Warsaw

5. Conclusions

Optical diffraction tomography applied for 3D measurement of refractive-index and birefringence distribution in optical microelements suffers from low dynamic range and high signal-to-noise ratio. These features caused by linearization used in tomographic reconstruction algorithms were studied by extensive numerical simulations for elements with various phase distributions. The limitations of ODT applicability for step and gradient-index objects have been determined. It was shown that for the objects having light converging or diverging properties the modified focusing (numerical or optical) should by introduced in tomographic reconstruction algorithm. This provides the results with reduced errors. In order to extend the dynamic range of ODT, new tomographic reconstruction algorithm was proposed for measurement of optical elements with the known design. This algorithm uses numerical back propagation of the measured scattered optical field in element design medium. It is shown that application of this algorithm allows 3D measurement of optical microelements having large deviation of refractive-index distribution.

Acknowledgements

The authors are grateful for the financial support within the European Network of Excellence in Micro-Optics NEMO and the statutory work performed at the Institute of Micromechanics and Photonics, Warsaw University of Technology.

References

1. M. Born and E. Wolf, *Principles of Optics*, Cambridge University Press, 1999.
2. C.V. Vest, "Interferometry of strongly refracting axisymmetric phase objects", *Appl. Opt.* **14**, 1601–1606 (1975).
3. T.C. Wedberg, J.J. Stamnes, and W. Singer, "Comparison of filtered backpropagation and backprojection algorithms for quantitative tomography", *Appl. Opt.* **34**, 6575–6581 (1995).
4. H. Aben, A. Errapart, L. Ainola, and J. Anton, "Photoelastic tomography for residual stress measurement in glass", *Opt. Eng.* **44**, 093601 (2005).
5. W.L. Howes and D.R. Buchele, "Optical interferometry of inhomogeneous gasses", *J. Opt. Soc. Am.* **56**, 1517–1528 (1966).
6. E. Wolf, "Determination of the amplitude and the phase of scattered fields by holography", *J. Opt. Soc. Am.* **60**, 18–20 (1970).
7. S.K. Mangal and K. Ramesh, "Determination of characteristic parameters in integrated photoelasticity by phase-shifting technique", *Opt. Lasers in Eng.* **31**, 263–278 (1999).
8. J. Hsieh, *Computed Tomography*, SPIE Press, Bellingham, 2003.
9. C.J. Dash, "One-dimensional tomography: a comparison of Abel, onion-peeling, and filtered backprojection methods", *Appl. Opt.* **31**, 1146–1152 (1992).
10. A.J. Devaney, "A filtered backpropagation algorithm for diffraction tomography", *Ultrasonic Imaging* **4**, 336–350 (1982).
11. P. Guo and A.J. Devaney, "Comparison of reconstruction algorithms for optical diffraction holography", *J. Opt. Soc. Am.* **A22**, 2338–2347 (2005).
12. C.M. Vest, "Tomography for the properties of materials that bend rays: a tutorial", *Appl. Opt.* **24**, 4089–4094 (1985).
13. N. Sponheim, L.J. Geljus, I. Johansen, and J.J. Stamnes, "Quantitative results in ultrasonic tomography of large objects using line sources and curved detector arrays", *IEEE Trans. Ultrason. Ferroelectr. Freq. Control.* **38**, 370–379 (1991).
14. K.H Brenner and W. Singer, "Light propagation through microlenses: a new simulation method", *Appl. Opt.* **32**, 4984–4988 (1993).
15. T. Kozacki, P. Kniazewski, and M. Kujawinska, "Photoelastic tomography for birefringence determination in optical microelements", *Fringe 2005*, *5th Int. Workshop on Automatic Processing of Fringe Patterns*, 226–229, Springer, 2005.
16. Q.H. Liu, "The PSTD algorithm: a time-domain requiring only two cells per wavelength", *Microwave Opt. Technol. Lett.* **15**, 158–165 (1997).
17. P. Kniazewski, T. Kozacki, M. Kujawinska, K. Szaniawska, and T.R. Woliński, "Application of the photoelastic tomography to measurement of refractive indices in optical anisotropic microelements", *Proc. SPIE* **6188**, 61880H (2006).
18. Y. Cheng and A.J. Devaney, "Inverse scattering and diffraction tomography in cylindrical background media", *J. Opt. Soc. Am. A* **23**, 1038–1047 (2006).